

Simulation of Gas-Cooled Fast-Reactor Cladding Melting and Resolidification in Cocurrent Flow

T.J.A. Scale

*Reactor Analysis and Safety Division,
Argonne National Laboratory, 9700 South Cass Avenue,
Argonne, Illinois 60439, U.S.A.*

D.T. Eggen

*Dept. of Mechanical and Nuclear Engineering,
The Technological Institute, Northwestern University,
Evanston, Illinois 60201, U.S.A.*

The behavior of stainless steel cladding during a loss-of-flow (LOF) accident in a Gas-Cooled Fast Reactor (GCFR) was investigated by performing simulation experiments with low melting-temperature alloys. The experiments were designed to simulate the melting and resolidification of fueled cladding subjected to downward coolant flow. The important experimental parameters were based on dimensional analysis of predicted GCFR coolant, cladding and fuel temperature histories.

The experiments used helium, argon, or air as coolants. The cladding material was either a 50/50-Pb/Sn or 76/24-Pb/Bi alloy. The simulant fuel was alumina with an internal nichrome heater. Films were taken of the experiments to classify the regimes of cladding motion as a function of the gas-coolant Reynolds and Weber numbers.

The cladding motion was seen to fall into several flow regimes. At zero flow, the cladding moved in a complicated sliding and teardrop-falling manner. As the gas Reynolds and Weber numbers were increased, draining, forced draining, and finally cladding entrainment and disintegration flows were observed. When Reynolds number is $\geq 12,900$ and the Weber number is ≥ 1.43 , cladding entrainment can be expected.

Experiments were performed to calculate the fraction of entrained cladding which would solidify on a simulant-alloy grid spacer. Two important correlations are:

1. The ratio of mass deposited on a grid spacer to the total mass escaping the test section decreases as the Reynolds number increases.
2. The mass fraction of escaped particulates of less than $210 \mu\text{m}$ size to the total escaped particulates increases as the coolant-cladding Weber number increases.

This implies the possibility of coolant-flow blockage during the LOF.

* Mr. Scale is currently in the Reactor Analysis and Safety Division at Argonne National Laboratory.

1. Introduction

During a loss of flow event in a Gas-Cooled Fast Reactor, with or without power shut-down, it is possible that the fuel cladding will melt and flow or be blown out of the reactor core region. It was a hypothesis at the initiation of experimental research several years ago that the cladding could be entrained and/or freeze on the grid spacers located along the core and blanket elements. Because of the difficulties of working with stainless steel clad fuel elements, our experiments have used simulant materials; namely, Pb-Sn and Pb-Bi eutectic alloys to simulate the cladding and heater rod of alumina as a fuel simulant. Early experiments [1] with multiple rod bundles and simulant grid spacers indicated that cladding, melted in the core region with modest amounts of superheat, did entrain and freeze in the blanket grid spacer. Later experiments [2,3] with full length fuel rods and a heater incorporating a chopped cosine power shape utilized single and triple simulant fuel rods with grid spacers. It was shown that the grid spacers in the core entrain and delay the passage of molten or particulate cladding from the "core" region and finally provided a nucleus to initiate flow blockage in the blanket region.

Concurrent with the experimental research analytical models were developed to correlate the data obtained with the simulant materials [4], and also to investigate the practical case of stainless steel-nuclear fuel systems [5]. During these developments, dimensional analysis techniques identified four major parameter groups of most importance to the simulation of a flow coastdown event at power. These are: The Reynolds number ($\rho_g Vd/\mu$); Weber number ($\sigma/D\rho_g V^2$); $C(\bar{T}_1 - \bar{T}_2)/h$; and $M(\text{escape})/M(\text{stuck})$; where ρ_g is the gas density; V , the gas velocity; D , the hydraulic diameter (heated); μ , the gas viscosity; σ , the interface surface tension between the liquid cladding and the gas; C , specific heat of the cladding and spacer; $(\bar{T}_1 - \bar{T}_2)$, the temperature difference of the average melting, moving cladding and the average temperature of the grid; h , the latent heat of fusion for the cladding and grid; $M(\text{escape})$ is the amount of molten or particulate cladding that passed through the grid and $M(\text{stuck})$ is that which was entrained or frozen on the grid.

The first two are important in characterizing the type of motion and the manner in which the cladding moved as a result of the loss of coolant event. These and the latter two are important in assessing the likelihood of flow blockage. Other parameter groups were evaluated and found to be less important as long as their values were reasonably approximate between the real system and the simulative system.

2. Characterization of Cladding Flow Regimes

Because of the complexity of the full length experiments and the difficulty in interpreting and controlling several different phenomena at once, "short" rod tests were initiated. These included a short (35 cm long and 0.67 cm diam) heater element clad with either Pb-Bi or Pb-Sn alloy over a 15 cm length. A gas flow channel was made of a heated glass tube, 28 cm long and 15.5 mm ID. A rubber hose connected to the top of the tube supplied flow-controlled coolant air. The glass channel was heated to simulate adjacent heated rods. The Pb-Bi cladding had an OD of 8.25 mm and an ID of 6.75 mm. The Pb-Sn alloy cladding had an OD of 8.1 mm and an ID of 6.8 mm. The configuration is shown in Fig. 1.

This apparatus was used to study the cladding flow characteristics on an abrupt reduction in flow of the air coolant, while the heater power remained constant. By analysis this technique of an abrupt flow reduction was shown to be equivalent to a fast ($\alpha=1$ sec) flow coastdown (as discussed later). Moving pictures were taken with a 16 mm camera at 64

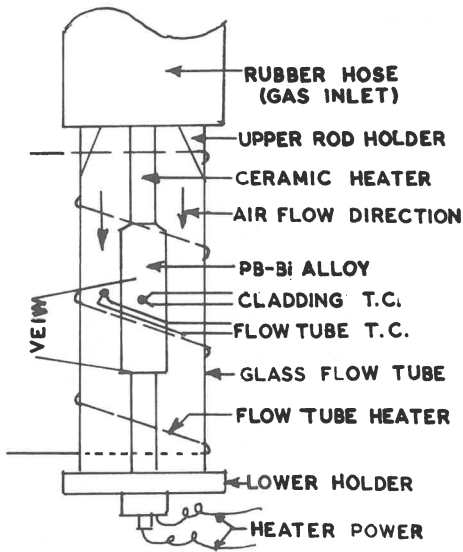


Fig. 1. Schematic of test section used in cladding motion experiments.

frames/sec.

The procedure for the tests was to adjust flow from two air sources such that the sum of the flow was the normal flow (70-90 m/s) for the rated power (250 to 300 w). One flow was adjusted to be that required for the specific test condition i.e., zero to 45 m/sec. The heater power was adjusted, the channel heater was energized, the camera and recorders were started and the main air valve was closed, leaving only the "drop" flow to cool the rod. Thermocouple, flow, and pressure data were recorded on magnetic tape for later diagnosis.

Three series of tests were run to characterize the melted cladding flow. Series 4 used Pb-Bi alloy and had a "drop flow" of 0m/sec, seven series 6 tests used Pb-Bi alloy cladding and covered a range of "drop flows" from 18 to 45 m/sec. Seven series 8 tests used Pb-Sn alloy cladding and ranged in flow from zero to 41 m/sec. See Table I.

A computer program was developed which could predict the fuel, cladding, and gas coolant temperatures for a variety of problems using different initial flow velocities, gas-coolant, flow coastdown rates, and fuel heating rates. The experimental model assumed that a dropped flow experiment would yield the same results as a flow coastdown. If the blanket cladding and core-cladding temperatures and the gas coolant velocity are the same for the two cases at the point where the cladding moves, it is expected that the two experiments will yield the same results. Results from a flow coastdown with $\alpha = 1 \text{ sec} [V = V_0 \exp(-\alpha t)]$ were compared with a flow drop calculation where the inlet velocity dropped from 84 m/s to 15 m/s. These results are shown in Table II. Correlation of important dimensionless parameters agree reasonably well. For cases when the α was changed to 5 and 25 seconds (slower coastdown), it was found that the amount of latent heat in the cladding increases significantly (see parameter $\pi-5$ in the third and fourth columns of Table II). It is seen that as α increases, the blanket cladding temperature increases to a point above the solidus thereby providing no heat sink to the core cladding as it enters the blanket region. Also since the latent heat in the core cladding increases (w_0) the probability of freezing in the blanket is further reduced and for $\alpha = 25\text{s}$ there is no possibility of refreezing in the blanket.

The zero flow tests in series 4 (test 1) and series 8 (test 4) where the air flow dropped abruptly from 53 m/s to 0 m/sec are characterized by two predominated modes of cladding motion. In Fig. 2a, a protusion of molten liquid from inside the cladding is falling in the annular space between the heater and channel wall. In Fig. 2b, motion results when a break in the cladding eventually occurs and a sleeve of the cladding slides down the heater.

TABLE I
VARIABLES IN THE SMALL LENGTH TESTS

Test #	Alloy	Type	Rod Htr. Power Watts	Glass Htr. Power Watts	Air Vel. m/s	Re	We
T-1	S-4	Pb-Bi	257	475	0	0	0
T-2	S-4	Pb-Bi	243	467	0	0	0
T-1	S-6	Pb-Si	284	634	18	8,000	6
T-2	S-6	Pb-Bi	290	612	26	12,400	1.31
T-3	S-6	Pb-Bi	290	634	32	15,200	1.97
T-4	S-6	Pb-Bi	290	792	37	17,500	2.62
T-5	S-6	Pb-Bi	318	862	45	22,000	3.95
T-7	S-6	Pb-Bi	300	792	32	15,300	1.97
T-1	S-8	Pb-Sn	280	594	28	12,900	1.43
T-2	S-8	Pb-Sn	280	614	19	8,600	.65
T-3	S-8	Pb-Sn	296	581	35	16,200	2.26
T-4	S-8	Pb-Sn	266	594	0	0	0
T-5	S-8	Pb-Sn	332	684	41	20,000	3.26
T-6	S-8	Pb-Sn	352	714	41	20,100	3.28
T-7	S-8	Pb-Sn	290	748	26	12,200	1.26

TABLE II
COMPARISON OF LOSS OF FLOW BY COASTDOWN OR FLOW DROP

	<u>Flow drop</u>	<u>Pump Coastdown</u>		
	Inlet velocity dropped from 84 m/s to 15 m/s	$\alpha = 1s$	$\alpha = 5 \text{ sec}$	$\alpha = 25 \text{ sec}$
Time to exceed 1385C in clad, s	3.3	4.8	13.0	44
\bar{T}_c , average cladding Temp., C	1391	1390	1397	1403
\bar{T}_B , average blanket Temp., C	980	1045	1309	1398
Average core, Re	12,300	12,100	19,700	24,500
Average core velocity, m/s	39.6	38.4	63.3	79.8
$w_o = \frac{T_c - 1385}{1410 - 1385}$.24	.20	.48	.72
$\frac{C_p (1385 - \bar{T}_B)}{w_o h_o s L} = \pi_5$	4.37	4.40	.41	--
$\frac{gL_c}{w_o h_o s L} = \pi_7$	4.5×10^{-5}	5.4×10^{-5}		
$\frac{V^2}{g D_h} = \pi_6$	2.3×10^4	2.2×10^4		
$\frac{v^2 \rho D_h}{\sigma} = \pi_9 (We)$	52.5	49.6		
$\frac{v^2 \rho t_{cladding}}{\sigma} = \pi_9^* (We^*)$	3.74	3.53	3.18	5.03

[Each figure includes four pictures drawn from frames taken .031 (in some cases .015) sec apart on the movie film record. Because of the quality of the pictures, the outline of the cladding, cladding fragments and droplets, and the heater and flow channel have been drawn with as much care as possible.]

Generally, since there is no force except gravity on the cladding at zero flow, the cladding is melted from the inside out until it becomes so weak as not to be able to support its weight. It then breaks and slides down. Subsequently the melted cladding on the inside surface flows out, forms droplets or whiskers, leaving a hollow shell behind.

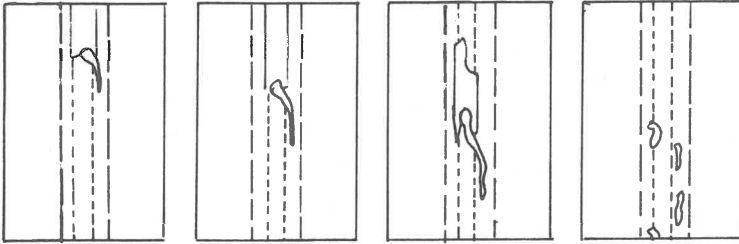


Fig. 2a
Series 4
Test 1
Vel. 0 m/s
Pb-Bi
frames 31 ms

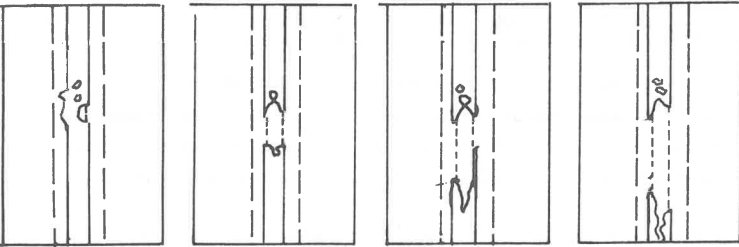


Fig. 2b
Series 8
Test 4
Vel. 0 m/s
Pb-Sn
frames 31 ms

Fig. 2. When the flow is reduced to zero, the cladding melts from the inside draining from "whiskers", and tubes of cladding slide down.

The next phase which characterizes the flow at intermediate velocities is seen in Fig. 3 for series 8 tests 2(3a) and 1(3b). In test 2 (Fig. 3a) at a flow of 19 m/s, a motion which we refer to as forced drainage occurs, although it is difficult to see in the few frames, the cladding melts from the inside out (as for the zero flow case) and the outer surface continually shrinks under the pressure of the gas flow, until only a very thin film remains which then breaks and falls. In Fig. 3b, the typical forced drainage characteristic of lower flows, except for a more rapid and pronounced tearing away of the droplet, produced from the liquid streams flowing from inside the cladding. In several tests in this flow regime, waves were noted to form (Fig. 3a) on the cladding surface. The crests then provided the force to break the cladding away and allow the drainage to start.

The last and most violent phase of the cladding motion is illustrated in Figs. 4 for Series 6 tests. The velocities represented at 32 m/s (Fig. 4a, test 3), 37 m/s (Fig. 4b, test 4), and 45 m/s (Fig. 4c, test 5). This flow regime is characterized by a violent tearing and fragmentation of the cladding as it weakens due to melting. The fragments are entrained in the flow stream and thrown through the channel. In Fig. 4a, one can see how quickly the cladding is stripped from the rod. It is clear that the cladding is not liquid but not really solid either. The mean temperature of the cladding was about 192 C which is

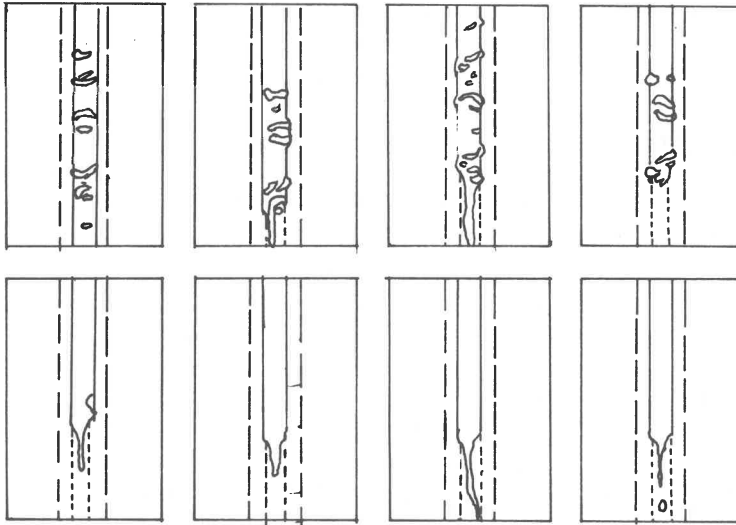


Fig. 3a
Series 8
Test 2
Ve. 19 m/s
Pb-Sn
frame 31 ms

Fig. 3b
Series 8
Test 1
Ve1. 28m/s
Pb-Sn
frames 31 ms

Fig. 3. At intermediate velocities ($Re < 12,900$) forced draining occurs. The coolant pressure squeezes melted cladding from inside tubing sheath. Waves form on surface.

in the phase transition region. We refer to this type of motion as entrainment. Fig. 4b shows even greater and earlier fragmentation and entrainment. In Fig. 4c the frames are only 15 ms apart and show the great violence which breaks up the cladding into small particles and finally is plastered to the inner surface of the flow channel to obscure any further data.

Based on observations made on the many feet of movie film from these and other tests, we propose that the transition from the forced drainage regime to the entrainment regime occurs at a Reynolds number $\geq 12,900$ and a Weber number ≥ 1.43 . These criteria are applicable for both Pb-Bi and Pb-Sn alloys and we also expect them to apply to other alloys including stainless steel.

3. Criteria for Channel Blockage Due to Grids

Another group of tests using a longer test section and incorporating a grid spacer in the simulated blanket region were done. The flow channel and "fuel" element were 52 cm long. The heater was wound in the ceramic rod over the upper 39.5 cm of length. The lower section representing the blanket received only 5% of the power/cm as the "core" region.

To evaluate the effect of the grid on particulate flow, two test series were run. In 10 series 10 tests the inlet pressure was maintained constant to simulate the lowering of the flow as the channel (grid) became blocked. In the 14 series 11 tests no pressure regulation was used and therefore the inlet pressure would rise as blockage occurred which could result in forcing out some of the particulates.

The test procedure was much the same as before except for the provision to regulate the inlet pressure in Series 10. The grid was weighed prior to the test. After the test the grid was again weighed and the increase was recorded as $M(\text{stuck})$. The amount of cladding penetrating the grid was also weighed and sized as $M(\text{escape})$. No correlation between the ratio $M(\text{escape})/M(\text{stuck})$ and Re is apparent in Series 10 where inlet pressure was held constant and consequently the flow velocity decreased due to partial blockage.

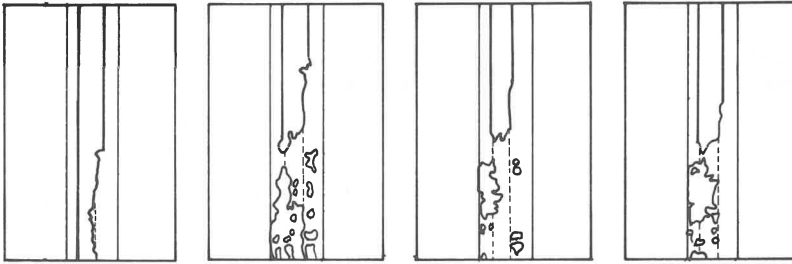


Fig. 4a
Series 6
Test 3
Vel. 32 m/s
Pb-Bi
frames 31 ms

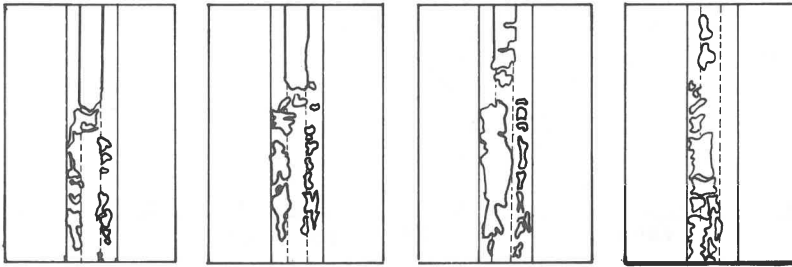


Fig. 4b
Series 6
Test 4
Vel. 37 j/s
Pb-Bi
Frames 31 ms

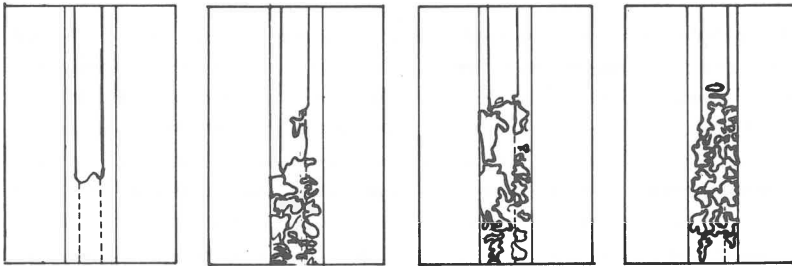


Fig. 4c
Series 6
Test 5
Vel. 45 m/s
Pb-Bi
Frames 15 ms

Fig. 4. At high coolant velocity ($Re > 12,900$), cladding is torn from heater, fragments (or explodes 4c), and is entrained.

Series 11 tests maintained constant flow conditions and therefore maintained the flow regime (forced drainage or entrainment) throughout. A small pressure spike was noted in most tests, but was less than 40% over pressure. A summary of results is shown in Table IV. One notes that all the tests are in the entrainment regime, i.e. $Re \geq 12,900$ and $We \geq 1.43$ (the gas velocity is a weighted average over the test period). In these tests the weight of particulates of mesh size less than 210μ was measured as well as the total mass escaping. Fig. 5a shows the correlation between $M(\text{stuck})/M(\text{escape})$ with Reynolds number. And Fig. 5b shows a correlation between $M(210\mu)/M(\text{stuck})$ and the Weber number.

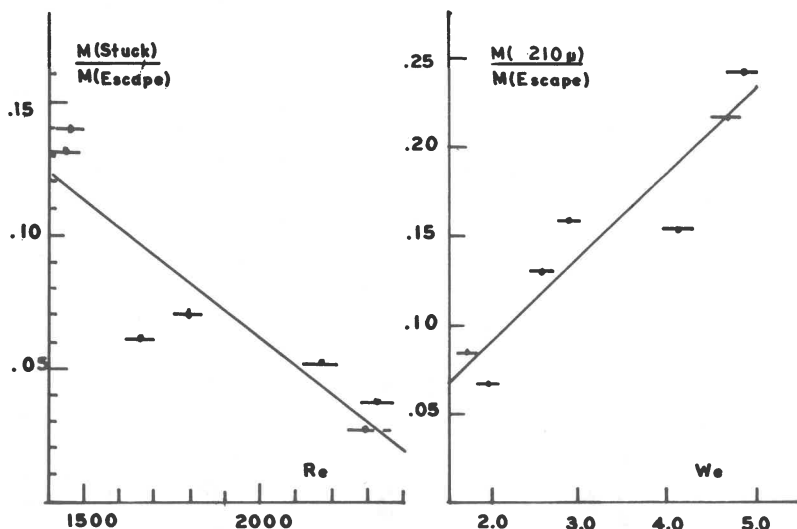


Fig. 5. Correlations on $M(\text{stuck})/M(\text{escape})$ vs Re and $M(< 210\mu)/M(\text{stuck})$ vs We

These graphs show a definite correlation between the parameters over the range of Re and We numbers considered. One must compare these numbers with those generated in the computer program to determine the similitude for a GCFR loss of flow case. At the bottom of Table IV are given the value calculated for $\alpha = 1, 5$ and 25 sec. It is seen that the Reynolds numbers in the tests provide good coverage and that several of the experiments are within the range stipulated by the computer output. The fact that some experiments have lower Weber numbers indicates that the computer predictions bias the size of particulates in a GCFR-LOF. The fact that the experimental numbers are greater than predicted by the computer means that more refreezing is expected in the experiments than in the actual system.

TABLE IV
CONSTANT FLOW TESTS SERIES 11 Pb-Bi ALLOY

Test #	N_{Re}	N_{We}	π_5^*	M_{ES}	M_{STUCK}	$\frac{M_{STUCK}}{M_{ES}}$	$M < 210\mu$	$\frac{M < 210\mu}{M_{ES}}$
				Grams	Grams		Grams	Grams
T-1	21,600	4.14	3.56	15.09	.79	.052	2.33	.154
T-4	14,600	1.95	2.82	12.23	1.72	.14	.81	.066
T-5	16,600	2.61	2.61	10.03	.61	.061	1.30	.130
T-6	17,900	2.87	2.87	13.61	.96	.070	2.19	.161
T-8	14,500	1.72	1.72	10.25	1.35	.131	.87	.085
T-11	23,000	4.67	4.67	13.23	.36	.027	2.89	.217
T-13	23,300	4.84	4.84	12.73	.48	.038	3.08	.242
$\alpha = 1$ sec	12,100	1.18	4.40					
$\alpha = 5$ sec	19,700	3.18	0.41					
$\alpha = 10$ sec	24,500	5.03	--					

$$* \pi_5 = \frac{C(\bar{T}_{cl} - T_{gr})}{w_o h}$$

4. Conclusions

Cladding flow in a loss of flow event can be characterized as (1) drainage and slipping at very low coolant velocities, (2) forced drainage at intermediate velocities, and (3) fragmentation and entrainment at high velocities. The data indicates that the transition from (2) to (3) occurs when $Re \geq 12,900$ and $We \geq 1.43$.

With entrained cladding flow, part of the particulates will stick by freezing on the colder blanket grid, depending on the Reynolds and Weber numbers, and if the sensible heat of the grid is large compared to the cladding latent heat (π_5 larger than 1). The following correlation is made for the amount of cladding that sticks to the grid to that which passes through:

$$\frac{M(\text{stuck})}{M(\text{escape})} = (0.27 \pm 0.05) - (0.10 \pm 0.30 \times 10^{-4})^* Re,$$

for $Re \geq 12,900$

A correlation is also made for the mass of small particulates passing to the total mass of particulates escaping the grid:

$$\frac{M(< 210 \mu)}{M(\text{escape})} = -(0.0013 \pm 0.028) + (.0467 \pm 0.0080)^* We$$

for $We \geq 1.41$.

5. References

- [1] Weber, Paul, "Cladding Motion Simulation in a GCFR-LOF Accident," M.S. Thesis, Northwestern University, 1975.
- [2] Eggen, D. T., Scale, T., Hsieh, S., "The Effects of Spacers on the Blockage of Coolant Channels in Clad Melting Accidents," Proc. 4th SMIRT Conf. - San Francisco, Aug. 1977.
- [3] Chu, N., Scale, T., Eggen, D. T., "Simulation of Cladding Melting and Resolidification in GCFR Under LOF Using Sn Alloy," Trans. Am. Nucl. Soc., Toronto, June, 1977.
- [4] Chu, N., and Eggen, D. T., "Simulation of Transient Freezing of Cladding in GCFR Blanket Channels," Proc. Intl. Conf. on Fast Reactor Safety and Related Physics, Chicago, Oct. 1976; CONF-761001.
- [5] Wehner, T. R., and Eggen, D. T., "Fuel Deformation in a Loss of Flow Accident in GCFR," Proc. 5th SMIRT Conf., Berlin, Aug. 1979.

N.B. This paper is based on the Ph.D. dissertation of Timothy Scale to Northwestern University, Evanston, Illinois 1978.